Rothamsted Research
Harpenden, Herts, AL5 2JQ

Telephone: +44 (0)1582 763133
Web: http://www.rothamsted.ac.uk/

Rothamsted Repository Download

A - Papers appearing in refereed journals

Lin, M. T., Occhialini, A., Andralojc, P. J., Devonshire, J., Hines, K. M., Parry, M. A. J. and Hanson, M. R. 2014. Beta-carboxysomal proteins assemble into highly organized structures in Nicotiana chloroplasts. *The Plant Journal.* 79 (1), pp. 1-12.

The publisher's version can be accessed at:

- https://dx.doi.org/10.1111/tpj.12536

The output can be accessed at: https://repository.rothamsted.ac.uk/item/8qyzy.

FEATURED ARTICLE

β-Carboxysomal proteins assemble into highly organized structures in *Nicotiana* chloroplasts

Myat T. Lin[1,†], Alessandro Occhialini[2,†], P. John Andralojc[2], Jean Devonshire[2], Kevin M. Hines[1], Martin A. J. Parry[2] and Maureen R. Hanson[1,*]

[1]*Department of Molecular Biology and Genetics, Cornell University, Ithaca, NY 14853, USA, and*
[2]*Plant Biology and Crop Science, Rothamsted Research, Harpenden, Herts AL5 2JQ, UK*

SUMMARY

The photosynthetic efficiency of C3 plants suffers from the reaction of ribulose 1,5-bisphosphate carboxylase/oxygenase (Rubisco) with O_2 instead of CO_2, leading to the costly process of photorespiration. Increasing the concentration of CO_2 around Rubisco is a strategy used by photosynthetic prokaryotes such as cyanobacteria for more efficient incorporation of inorganic carbon. Engineering the cyanobacterial CO_2-concentrating mechanism, the carboxysome, into chloroplasts is an approach to enhance photosynthesis or to compartmentalize other biochemical reactions to confer new capabilities on transgenic plants. We have chosen to explore the possibility of producing β-carboxysomes from *Synechococcus elongatu*s PCC7942, a model freshwater cyanobacterium. Using the agroinfiltration technique, we have transiently expressed multiple β-carboxysomal proteins (CcmK2, CcmM, CcmL, CcmO and CcmN) in *Nicotiana benthamiana* with fusions that target these proteins into chloroplasts, and that provide fluorescent labels for visualizing the resultant structures. By confocal and electron microscopic analysis, we have observed that the shell proteins of the β-carboxysome are able to assemble in plant chloroplasts into highly organized assemblies resembling empty microcompartments. We demonstrate that a foreign protein can be targeted with a 17-amino-acid CcmN peptide to the shell proteins inside chloroplasts. Our experiments establish the feasibility of introducing carboxysomes into chloroplasts for the potential compartmentalization of Rubisco or other proteins.

Keywords: β-carboxysome, synthetic biology, photosynthesis, CO_2 concentration mechanism, chloroplast engineering, bacterial microcompartment, *Nicotiana benthamiana*.

INTRODUCTION

Intracellular compartmentalization is a general strategy used by organisms to carry out metabolic reactions more efficiently. Several bacteria enclose enzymes within proteinaceous polyhedral bodies, known as bacterial microcompartments (BMCs; Bobik, 2006; Yeates *et al.*, 2008). These microcompartments allow the hosts to overcome unfavorable or challenging metabolic pathways by sequestering volatile or toxic reaction intermediates, or by concentrating a critical substrate nearby an enzyme that has a slow turnover and low affinity for that substrate. Despite their diverse functions, these microcompartments share a common set of homologous protein subunits, which make up the outer shells in a fashion similar to viral capsids (Yeates *et al.*, 2011).

The β-carboxysome from the freshwater cyanobacterium *Synechococcus elongatus* PCC7942 is perhaps the best-characterized bacterial microcompartment. It contains two enzymes fundamental to photosynthesis, namely ribulose 1,5-bisphosphate carboxylase/oxygenase (Rubisco) and carbonic anhydrase, and forms an important part of the cyanobacterial CO_2-concentrating mechanism (CCM; Yeates *et al.*, 2008; Rae *et al.*, 2013). Although essential to photosynthesis, Rubisco catalyzes two competing reactions involving the enediol form of ribulose-1,5-bisphosphate (RuBP). These are the productive carboxylation of RuBP by CO_2 and the wasteful oxygenation of RuBP by molecular oxygen, initiating photorespiration (Long, 1991). Carboxysomes increase the concentration of CO_2 around the cata-

lytic site of Rubisco, promoting the carboxylase activity and consequently suppressing the undesired reaction with oxygen (Cannon *et al.*, 2001; Price *et al.*, 2008; Whitney *et al.*, 2011).

A reasonable model for the arrangement of protein components in this β-carboxysome has been proposed (Rae *et al.*, 2013). The protein constituents of β-carboxysomes can be broadly classified as components involved in the formation of either the icosahedral shell or the internal structure. The shell is composed of multiple copies of single BMC domain proteins (Pfam00936), such as CcmK2, CcmK3 and CcmK4, and tandem BMC domain proteins (CcmO and CcmP), which contain two tandem repeats of BMC domains (Kinney *et al.*, 2011; Yeates *et al.*, 2011). The crystal structures of single and tandem BMC proteins showed that they form hexameric and pseudo-hexameric units, respectively, which oligomerize, forming the facets of the carboxysome shell (Kerfeld *et al.*, 2005; Tanaka *et al.*, 2009; Cai *et al.*, 2013). Another component of the shell, CcmL, contains a Pfam03319 protein domain. The crystal structure revealed that CcmL is able to form pentamers, and is thought to define the vertices between adjacent facets in the icosahedral shells (Tanaka *et al.*, 2008; Keeling *et al.*, 2014). These shell proteins are distinguished by their pores, which have different sizes and properties, and are believed to regulate the flux of metabolites into and out of the carboxysome (Kinney *et al.*, 2011).

The proteins encoded by *ccmM* and *ccmN* participate in the internal organization of β-carboxysomes. In *S. elongatus*, CcmM is present in two isoforms, a 58-kDa isoform (CcmM58) and a shorter 35-kDa isoform (CcmM35), which is synthesized from an internal ribosome entry site (Price *et al.*, 1998; Long *et al.*, 2005). CcmM58 has a C-terminal domain containing three copies of a protein domain similar to the small subunit of Rubisco (SSU-like domain) and an N terminus similar to γ-carbonic anhydrase, whereas CcmM35 contains only three SSU-like domains (Price *et al.*, 1993; Ludwig *et al.*, 2000). CcmM58 localizes immediately below the shell and has been shown to interact with the shell proteins such as CcmK2, as well as the internal components such as CcmN, Rubisco and carbonic anhydrase (Cot *et al.*, 2008; Long *et al.*, 2010; Kinney *et al.*, 2012). In contrast, CcmM35 is believed to be involved in the organization of Rubisco within the lumen of the β-carboxysome (Rae *et al.*, 2013). CcmN is another essential protein that recruits the shell components to a nucleus of Rubisco complexes during the assembly of new carboxysomes (Cameron *et al.*, 2013). The CcmN protein is characterized by the presence of an N-terminal domain, which interacts with CcmM58, and an approximately 20-amino-acid C-terminal peptide, which interacts with CcmK2 (Kinney *et al.*, 2012).

One possible strategy to enhance photosynthesis is to transfer components of a cyanobacterial CCM into the chloroplasts of C3 crops, in order to increase photosynthetic carbon fixation and reduce photorespiration (Price

et al., 2013; Zarzycki *et al.*, 2013). A recent theoretical analysis estimated that the engineering of carboxysomes into chloroplasts in combination with the addition of a bicarbonate ion transporter and the removal of stromal carbonic anhydrase could increase the crop yield by over 30% (McGrath and Long, 2014). Despite the great potential of carboxysomes for improved carbon-fixing efficiency in higher plants, there has been no report so far on the heterologous expression of proteins from the β-carboxysome or other BMCs in eukaryotic organisms.

In this work, we use a transient expression method to explore the possibility of transferring components of β-carboxysomes from *Synechococcus* PCC7942 into plant chloroplasts. Agroinfiltration of *Nicotiana benthamiana* leaves gave rise to high levels of protein expression, demonstrating that carboxysomal proteins can be produced in plant cells and correctly targeted into the chloroplast stroma when fused to a chloroplast transient peptide. The application of both fluorescence and transmission electron microscopy, in combination with immunogold labeling, enabled the visualization of assemblies of carboxysomal proteins in the chloroplast stroma.

RESULTS

All carboxysomal proteins expressed in this study were fused with the N-terminal chloroplast transit peptide from the Arabidopsis *recA* gene (Köhler *et al.*, 1997). Imaging analyses indicate that all the proteins were correctly targeted to chloroplast stroma.

Transient expression of CcmK2-YFP in *N. benthamiana* leaves

When yellow fluorescent protein (YFP)-tagged CcmK2 (CcmK2-YFP) was expressed and targeted to the chloroplasts of *N. benthamiana*, elongated structures were visualized by fluorescent microscopy (Figure 1a). Co-expression of CcmK2-YFP with other carboxysomal proteins did not alter these elongated fluorescent signals. We hypothesize that fusing YFP to the much smaller CcmK2 protein causes the CcmK2 subunits to assemble incorrectly, leading to these elongated structures and preventing proper interactions with other carboxysomal proteins. Hence, subsequent experiments were performed with CcmK2 lacking a YFP tag.

Transient expression in *N. benthamiana* leaves of CcmO, CcmK2, CcmL and CcmM58

When CcmO-YFP was targeted to chloroplasts, diffuse YFP signals were observed; alternatively, in some cases, polar aggregations were seen, probably because of very high protein levels (Figure 1b,c). We co-expressed CcmO-YFP with each of the other β-carboxysomal shell proteins, namely CcmK2, CcmK3, CcmK4 and CcmL. We found that only in the presence of CcmK2 was CcmO-YFP able to produce punctate fluorescent loci (Figure 1d,e), indicating the
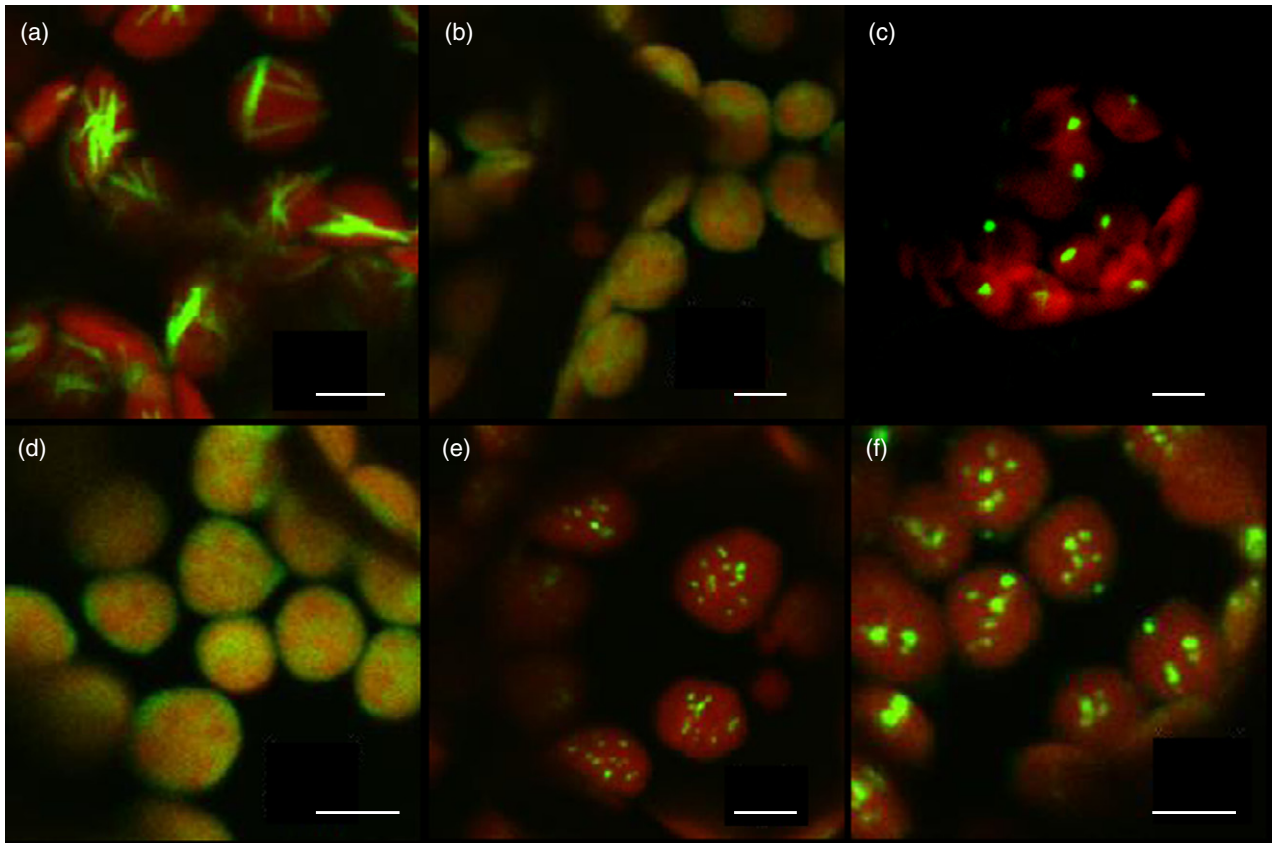
Figure 1. Confocal image of *Nicotiana benthamiana* leaf cells transiently expressing stroma-targeted YFP-tagged β-carboxysomal shell proteins. (a) CcmK2-YFP by 35SS promoter. (b, c) CcmO-YFP by 35SS promoter. (d) CcmO-YFP by 35SS promoter and CcmL by ubiquitin-10 promoter. (e) CcmO-YFP by 35SS promoter and CcmK2 by ubiquitin-10 promoter. (f) CcmO-YFP by 35SS promoter, CcmK2 by ubiquitin-10 promoter and CcmL by ubiquitin-10 promoter. Green, YFP fluorescence; red, chlorophyll autofluorescence. Scale bars: (a–f) 5 μm.

possible assembly of CcmK2 and CcmO-YFP. Punctate fluorescent signals were consistently produced when additional proteins such as CcmL and CcmM58 were co-expressed with CcmK2 and CcmO-YFP (Figure 1f).

In order to further resolve the structures formed by these punctate signals, the plant material was characterized at high resolution by transmission electron microscopy (TEM). Two different protocols of preparation of plant tissue were used: conventional chemical fixation at 20°C; and high-pressure freeze fixation (HPF)/freeze substitution in combination with immunogold labeling. In leaves expressing CcmO-YFP alone, large protein aggregates were observed (Figure 2a,d). Interestingly, when CcmO-YFP was expressed in combination with CcmK2, protein arrays organized into parallel linear structures were observed (Figure 2b,e). This result indicates that CcmO-YFP is not able to self-assemble into discrete structures, but when CcmK2 is present, the two carboxysomal proteins can interact, forming ordered assemblies - possibly sheets or stacked arrays of carboxysomal facets. Immunolabeling experiments using an anti-GFP antibody conjugated to 10-nm gold particles supported the pres-

ence of carboxysomal proteins in these structures (Figure 2d,e).

When we expressed another component of the shell, CcmL-YFP, along with CcmO-YFP and CcmK2, circular structures were observed (Figure 2c,f–i). The same outcome was observed using either form of sample preparation: conventional chemical fixation or HPF fixation. Immunogold experiments using anti-GFP (Figure 2f,g), anti-CcmK2 (Figure 2h) and anti-CcmO (Figure 2i) antisera confirmed the presence of CcmO and CcmK2 in these circular structures.

A size determination and a schematic representation of these structures are illustrated in Figure 3. They are round and slightly elongated, but some angular structures have been observed in high-quality plant material fixed by HPF (Figure 2g). They measure 100–110 nm in length and 80–90 nm in width. These carboxysome-like structures are surrounded by a double shell, with a space in between. The external shell measures about 5–6 nm in thickness, which is a value similar to that reported for a β-carboxysome shell (Kaneko *et al.*, 2006). In contrast, the structure of the second shell is difficult to resolve because it appears less thick and
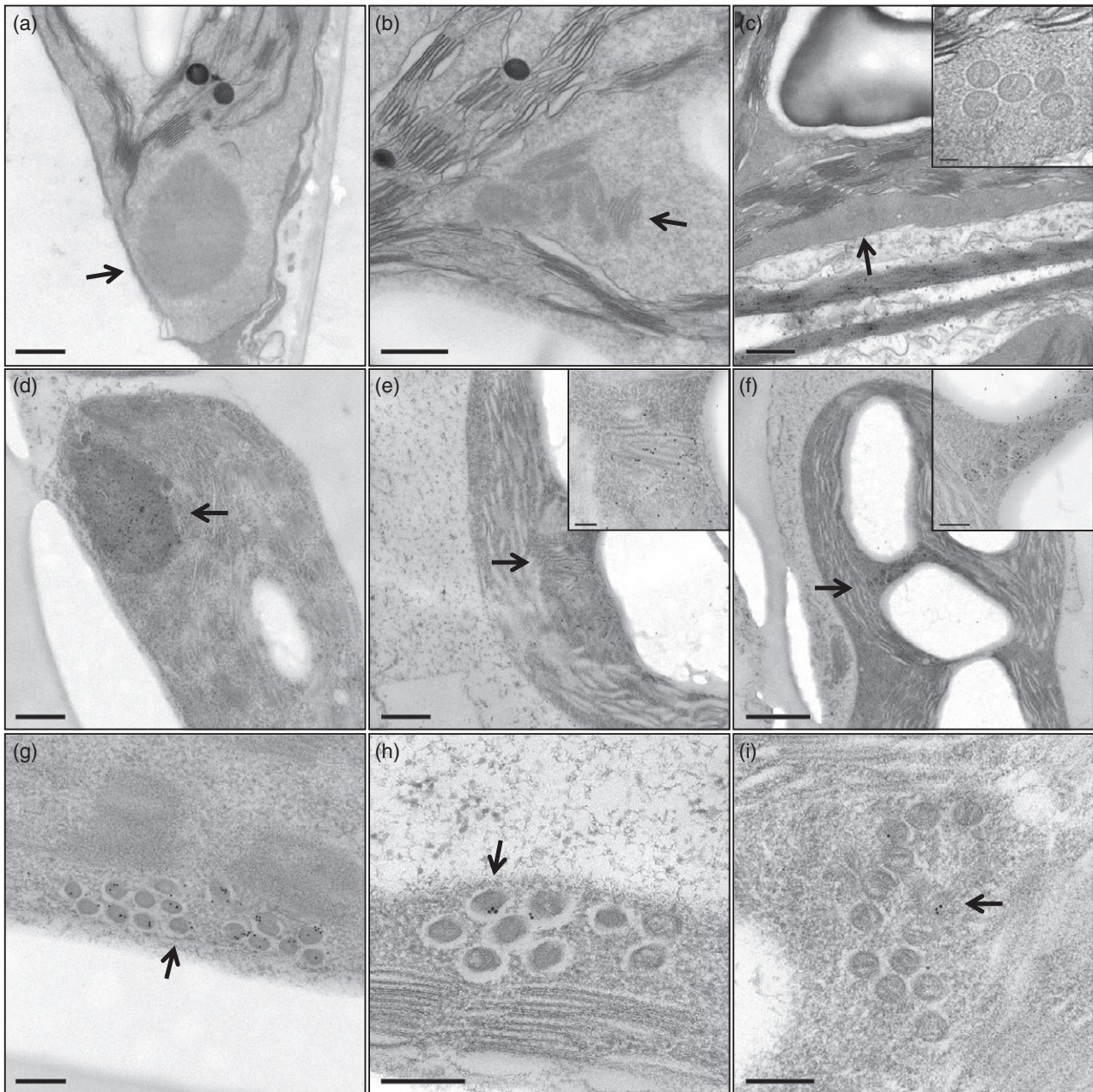
Figure 2. Electron micrograph of ultrathin sections of leaf mesophyll cells from agroinfiltrated *Nicotiana benthamiana* expressing the indicated carboxysomal proteins: (a, d) CcmO-YFP. (b, e) CcmO-YFP and CcmK2. (c, f–i) CcmO-YFP, CcmK2 and CcmL-YFP. Images showing different structures within the chloroplast stroma: (a, d, black arrows) protein aggregates; (b, e, black arrows) protein aggregates organized in parallel line structures; (c, f–i, black arrows) circular structures resembling a carboxysome shell. (a–c) Leaf tissue prepared by normal chemical fixation. (d–i) Leaf tissue prepared by high-pressure freeze fixation (HPF) in combination with immunogold labeling: (d–g) GFP labeling; (h) CcmK2 labeling; (i) CcmO labeling. A secondary antibody conjugated with 10-nm gold particles was used for the labeling. Scale bars: (a–e) 500 nm; (f) 1 μm; (g–i) 200 nm; (inset in c) 50 nm; (inset in e) 100 nm; (inset in f) 200 nm.

disorganized. An inner cavity surrounded by the double shell constitutes the internal part of the circular structure.

In the same plant material (expressing CcmO-YFP, CcmK2 and CcmL-YFP), other types of structures were observed as well as the round structures described above (Figure 4). Elongated (Figure 4a,d) and disorganized structures (Figure 4b,e) were observed, which probably result from different ratios of carboxysomal proteins (CcmO-YFP,

CcmK2 and CcmL-YFP), the proportions of which are likely to be heterogeneous within agroinfiltrated leaves. The presence of structures that are intermediate between a round and elongated shape may also reflect the importance of having an optimal ratio of carboxysomal proteins for carboxysome biogenesis (Figure 4c,f).

In plant material expressing CcmM58-YFP in combination with CcmO-YFP and CcmK2, round structures were

Figure 3. (a) Schematic representation of a circular structure. (b) High magnification of a circular structure in the chloroplast stroma of a mesophyll cell from agroinfiltrated *Nicotiana benthamiana* expressing CcmO-YFP, CcmK2 and CcmL-YFP. Leaf tissue prepared by normal chemical fixation. Scale bar: 50 nm.
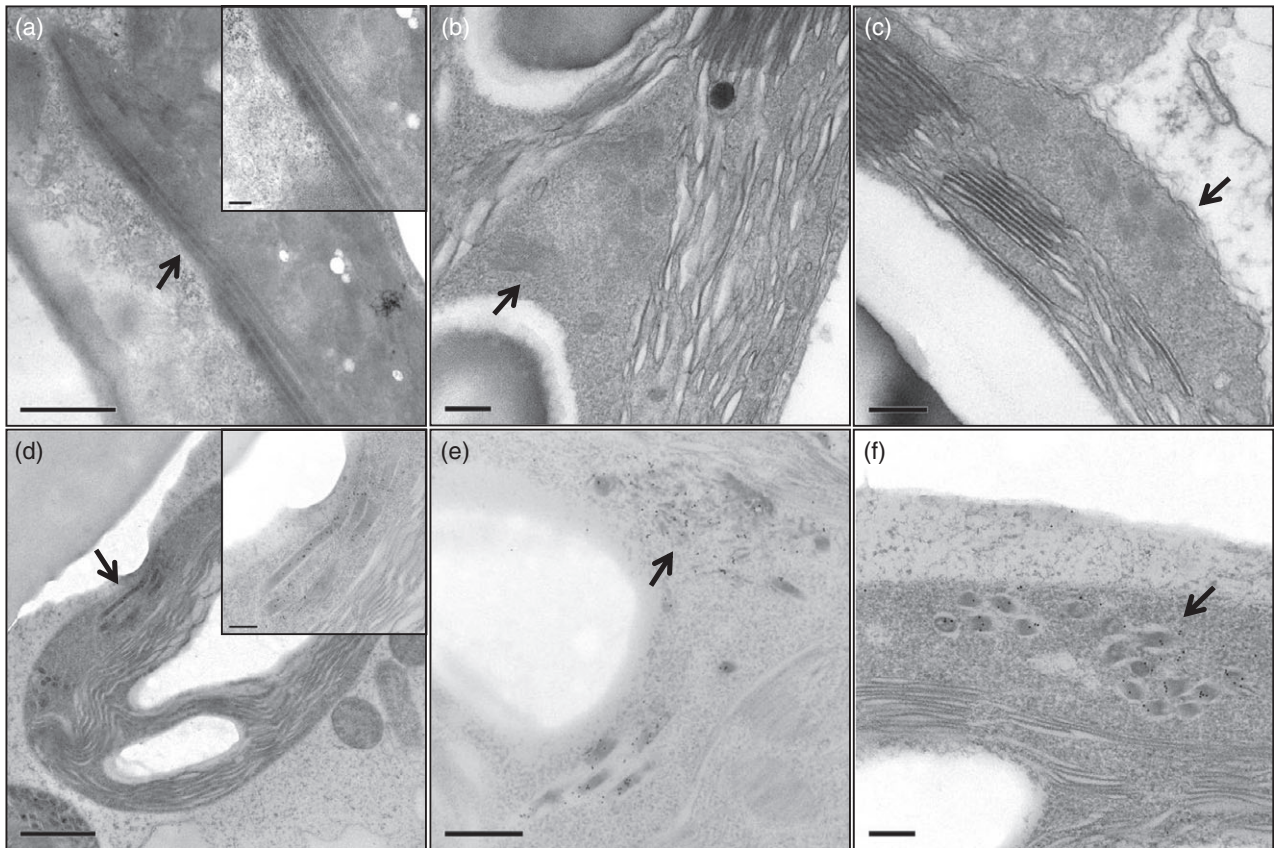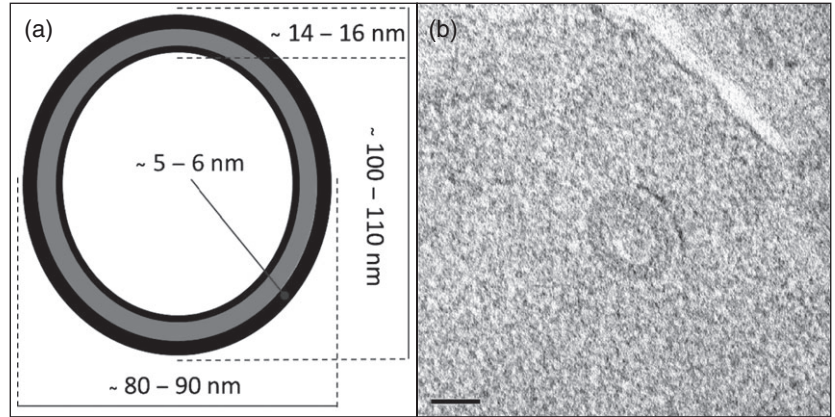

Figure 4. Electron micrograph of ultrathin sections of leaf mesophyll cells from agroinfiltrated *Nicotiana benthamiana* expressing CcmO-YFP, CcmK2 and CcmL-YFP. Images showing different structures within the chloroplast stroma: (a, d, black arrows) elongated structures; (b, e, black arrows) disorganized structures; (c, f, black arrows) intermediate structures. (a–c) Leaf tissue prepared by normal chemical fixation. (d–f) Leaf tissue prepared by high-pressure freeze fixation (HPF), in combination with immunogold labeling. An antibody against GFP and a secondary antibody conjugated with 10-nm gold particles were used. Scale bars: (a, d) 1 μm; (b, c, f) 200 nm; (e) 500 nm; (insets in a and d) 200 nm.

observed (Figure 5a). Immunolabeling experiments using antibodies against GFP (Figure 5b), CcmK2 (Figure 5c), CcmO (Figure 5d) and CcmM58 (Figure 5e) confirmed the presence of all these proteins. This result supports the

interpretation that sheets of CcmO-YFP/CcmK2 proteins form complex structures in the presence of CcmM58. In addition to the round structures, elongated structures were observed in some chloroplasts in plants agroinfiltrated

with constructs expressing CcmM58-YFP, CcmO-YFP and CcmK2 (Figure 5f,g). The elongated structures were organized into semicrystalline arrays of parallel lines, spaced 8–9 nm apart, that intersect, forming a net structure (Figure 5f,g). A similar organization of carboxysomal proteins in β-carboxysomes has been described by others (Kaneko *et al.*, 2006). Immunolabeling experiments using antibodies against GFP, CcmK2, CcmO and CcmM58 also confirmed the presence of these carboxysomal proteins in elongated structures (Figure S1).

In plant material expressing CcmO-YFP, CcmK2, CcmL and CcmM58-YFP together, we observed the same type of carboxysome-like and elongated structures described for the CcmO-YFP, CcmK2 and CcmM58-YFP plant material
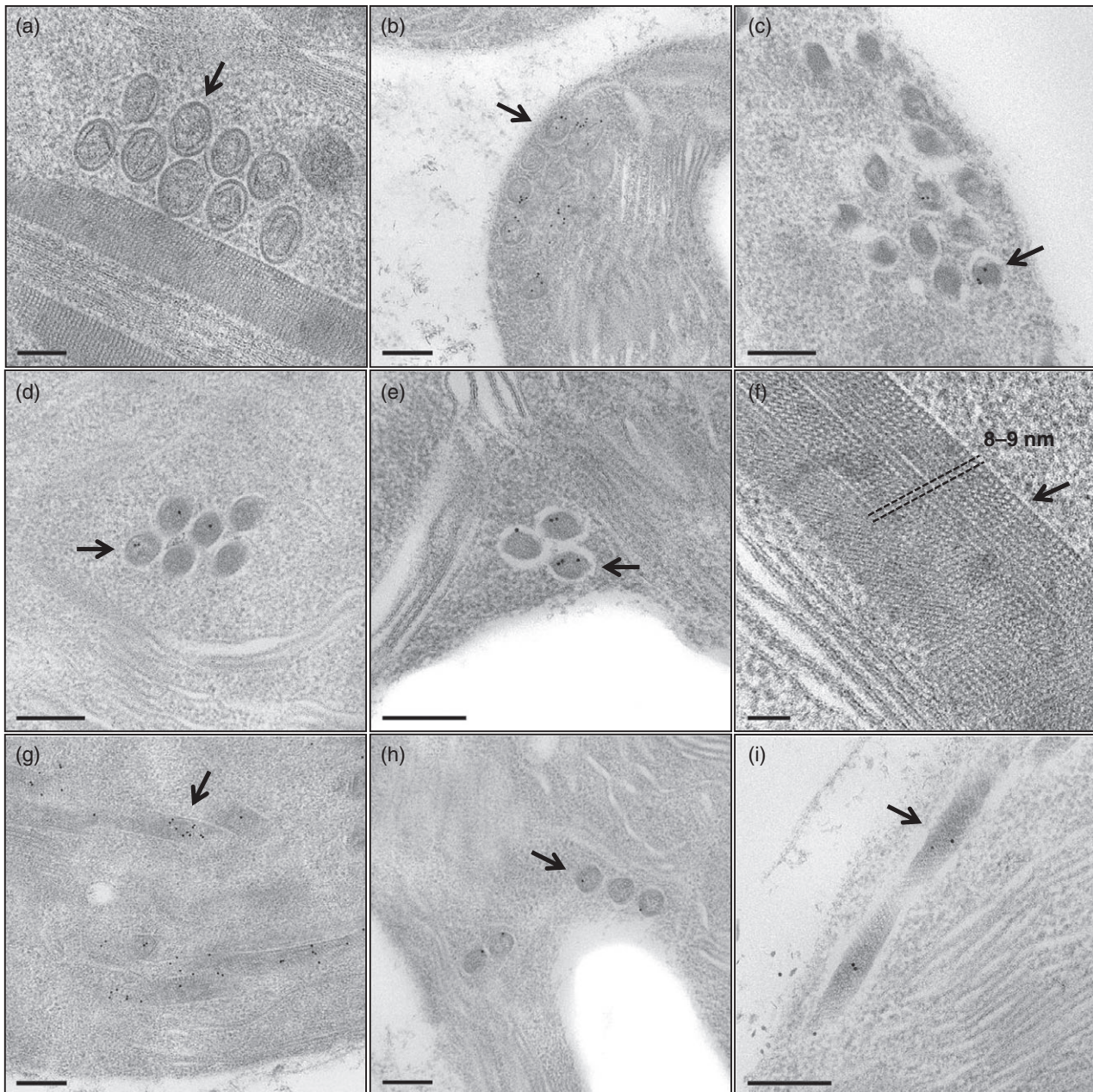

Figure 5. Electron micrograph of ultrathin sections of leaf mesophyll cells from agroinfiltrated *Nicotiana benthamiana* expressing the indicated carboxysomal proteins: (a–g) CcmO-YFP, CcmK2 and CcmM58-YFP; (h, i) CcmO-YFP, CcmK2, CcmL and CcmM58-YFP. (a–e, h, black arrows) Images showing circular structures resembling a carboxysome shell; (f, g, i, black arrows) images showing elongated structures (parallel lines, spaced 8–9 nm apart, and organized forming a net structure are indicated). Leaf tissue prepared by high-pressure freeze fixation without immunogold labeling (a, f), and in combination with immunogold labeling (b–e, g–i). Different antibodies against carboxysomal proteins were used: (b, g–i) GFP labeling; (c) CcmK2 labeling; (d) CcmO labeling; (e) CcmM58 labeling. A secondary antibody conjugated with 10-nm gold particles reacted with the primary antibodies. Scale bars: (a) 100 nm; (b–e, g-i) 200 nm; (f) 50 nm.

(Figure 5h,i). Immunolabeling experiments with an anti-GFP antibody supported the presence of the carboxysomal proteins.

CcmN contains a 17-amino-acid peptide that can target YFP to the structures formed by CcmK2/CcmO-YFP

We also co-expressed CcmN, an internal protein of β-carboxysomes, with CcmK2 and CcmO. When expressed alone, CcmN-CFP gave diffuse CFP signals (Figure 6a). When CcmN-CFP was co-expressed with CcmK2 and CcmO-YFP, both CcmN-CFP and CcmO-YFP gave punctate signals, which co-localized to the same areas in chloroplasts, suggesting that CcmN was able to associate with the structures composed of CcmK2 and CcmO-YFP (Figure 6b–d). When we removed the C-terminal 17-amino-acid peptide of CcmN and fused the truncated CcmN to CFP, the resulting protein fusion, CcmNd17-CFP, no longer co-localized with the punctate structures of CcmK2 and CcmO-YFP (Figure 6e,f). This finding is consistent with a recent report that demonstrated that CcmN interacts with CcmK2 through its C-terminal 17-amino-acid peptide (CcmN17; Kinney *et al.*, 2012).

In order to test the ability of the CcmN17 peptide to target a foreign protein to the structures formed by CcmK2 and CcmO-YFP, we co-expressed CcmK2 and CcmO-YFP with CcmN17-CFP, where the CFP was fused to the C termi-nus of CcmN17. But the CcmN17-CFP fluorescent signals were diffuse and did not co-localize with the punctate signals of CcmO-YFP (Figure S2). We hypothesize that the CFP fused to the C terminus of CcmN17, or that the 15-amino-acid scar peptide that remained at the N terminus of CcmN17, after the truncation of the chloroplast transit peptide, interfered with the interaction between CcmN17 and CcmK2. When we fused the N17 C-terminal peptide and YFP to the N terminus of CcmN17 and co-expressed it with CcmK2 and CcmO-CFP, both YFP-CcmN17 and CcmO-CFP fluorescent signals co-localized to punctate spots within chloroplasts (Figures 6g,h). Thus, the C-terminal 17-amino-acid peptide of CcmN (CcmN17) is critical for the binding of CcmN to the structures of CcmK2 and CcmO-YFP, and the CcmN17 peptide by itself is enough to target a foreign protein to the shell proteins of β-carboxysomes; however, we were not able to observe the formation of any specific structures in the leaf tissues expressing CcmN or CcmN17 with CcmK2 and CcmO by TEM (Figure S3).

DISCUSSION

In this study, we used the well-established agroinfiltration technique to express transiently several protein components of the β-carboxysome in chloroplasts of *N. benthamiana*. We fused several of these proteins with YFP or CFP, which allowed us to monitor the formation of protein
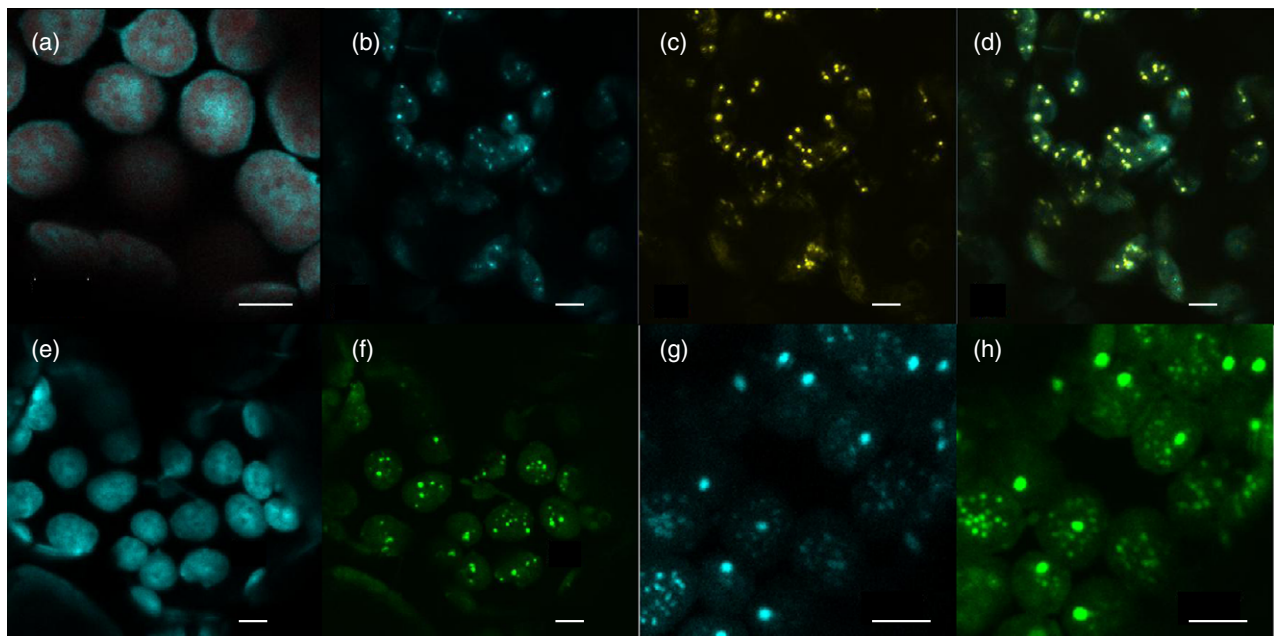

Figure 6. Confocal image of *Nicotiana benthamiana* leaf cells transiently expressing stroma-targeted CcmK2, CcmO and CcmN to determine co-localization. (a) CcmN-CFP by 35SS promoter. CFP fluorescence is shown in cyan and chlorophyll autofluorescence is shown in red. (b–d) CcmN-CFP by 35SS promoter, CcmK2 by ubiquitin-10 promoter and CcmO-YFP by MAS promoter. Individual CFP (b, in cyan) and YFP (c, in yellow) channels, as well as the merged channel (d, CFP in cyan and YFP in yellow), from the same region are shown. (e, f) CcmNd17-CFP by 35SS promoter, CcmK2 by ubiquitin-10 promoter and CcmO-YFP by MAS promoter. Individual CFP (e, in cyan) and YFP (f, in green) channels of the same leaf section are shown. (g, h) CcmO-CFP by 35SS promoter, CcmK2 by MAS promoter and YFP-CcmN17 by ubiquitin-10 promoter. Individual CFP (g, in cyan) and YFP (h, in green) channels of the same leaf section are shown. Scale bars: (a–h) 5 μm.

assemblies at the resolution of visible light. We found that fusing YFP to a much smaller shell protein of β-carboxysome, CcmK2, gave rise to elongated structures, and that co-expressing it with other shell proteins did not seem to alter these elongated structures. CcmK2 is the major shell component of β-carboxysomes, and has a high tendency to self-polymerize (Samborska and Kimber, 2012). YFP fusion is likely to cause distortion in the assembly of CcmK2 subunits, leading to artificially elongated structures, and preventing CcmK2 from forming normal interactions with other carboxysomal proteins. It was recently reported that CcmK2-YFP by itself could not substitute for the native unlabeled protein in the Δ*ccmK2* cyanobacterial strain, and that it could only interact with other carboxysomal components in the presence of unlabeled CcmK2 (Cameron *et al.*, 2013). Thus, the subsequent experiments were carried out without YFP fused to CcmK2. Although we did not observe any interference with the proper protein–protein interactions with YFP fused to other components, such as CcmO and CcmM58, we should caution that such fusions might disrupt other structural or functional aspects of β-carboxysomes. Fluorescent protein-labeled CcmK4 and RbcL in previous studies did not disrupt the structure or function of carboxysomes, as long as unlabeled versions were also present (Cameron *et al.*, 2013; Chen *et al.*, 2013).

Probably because of non-specific interactions, large protein aggregates were observed in agroinfiltrated *N. benthamiana* leaves expressing the fluorescently tagged carboxysome shell protein, CcmO-YFP, whereas co-expression of CcmK2 and CcmO-YFP gave rise to more organized, parallel structures. CcmO and CcmK2 are presumably the main components in the formation of the faces of the carboxysome shell (Rae *et al.*, 2012). Evidently CcmO-YFP alone is not able to self-assemble in a recognisable fashion, but in the presence of CcmK2, the two proteins can polymerize to form sheets that could represent arrays of shell faces. This finding is in agreement with a recent report suggesting that CcmO was unable to assemble with other components in the absence of CcmK2 (Cameron *et al.*, 2013).

When we added CcmL-YFP, the component involved in the formation of vertices of carboxysome shells (Tanaka *et al.*, 2008), round structures resembling carboxysome shells were observed. This result supports the notion that CcmL provides the requisite curvature for the formation of the icosahedral structure of the carboxysome, and is in line with recent work suggesting that CcmK2, CcmO and CcmL constitute the minimal structural determinants of the outer shells of β-carboxysome (Rae *et al.*, 2012). Circular structures that we observed in chloroplasts appear to be defined by a double shell, which contains an internal cavity. Probably the presence of a double shell represents a thermodynamically stable conformation of a combination

of CcmO-YFP, CcmK2 and CcmL-YFP in the absence of the other internal components, such as the cyanobacterial Rubisco. Indeed, CcmK2 has recently been shown to form a double-layered shell in the absence of other protein components (Samborska and Kimber, 2012).

These carboxysome-like structures are more frequently round and smaller than a normal β-carboxysome shell, but in some cases internal angular structures have been noted in particularly well-preserved plant preparations observed using the HPF fixation technique (Figure 2g). The oval-shaped structures measure 100–110 nm in length and 80–90 nm in width, whereas the diameter of a β-carboxysome from *Synechococcus* PCC7942 is ~175 nm (Rae *et al.*, 2013). The smaller size and less angular architecture of the outer shell are probably caused by the absence of other important components of the shell and of the carboxysome interior. It has been demonstrated recently that cyanobacterial Rubisco plays a central role in carboxysome nucleation, together with the two isoforms of CcmM, during the biogenesis of β-carboxysomes (Cameron *et al.*, 2013; Chen *et al.*, 2013). Only after nucleation does the shell form around this 'procarboxysome' via interactions with CcmN, which links the shell to the internal parts (Cameron *et al.*, 2013). This recently uncovered assembly process distinguishes β-carboxysome from other bacterial microcompartments, such as α-carboxysome and propanediol utilization metabolosome, which are generally known to be able to form empty compartments in the absence of lumen proteins (Menon *et al.*, 2008; Parsons *et al.*, 2010; Choudhary *et al.*, 2012). Nevertheless, at high concentration levels CcmK2 was able to form well-defined bodies ranging from 100 to 300 nm in size, and could interact with CcmL *in vitro* (Keeling *et al.*, 2014). The spherical structures observed in this study are more uniform in size and appear more organized, probably because of the presence of additional components, such as CcmO and CcmM58.

In *N. benthamiana* leaves expressing the three carboxysomal proteins CcmO-YFP, CcmK2 and CcmL-YFP, elongated structures and disorganized structures were also observed (Figures 5h,i and S1d–f). These are probably the result of different ratios of the three carboxysomal proteins. The quantity of each protein expressed transiently from T-DNA will vary in different cells, depending on how much T-DNA from each strain enters the cell as well as how much RNA is transcribed and translated. Furthermore, different carboxysomal proteins may vary in stability. We speculate that elongated structures are the result of CcmO-YFP and CcmK2 polymerization in the presence of suboptimal quantities of CcmL. In contrast, perhaps when CcmL is present at an appropriate concentration, carboxysome-like structures can be formed. This result is supported by studies performed in cyanobacteria where elongated carboxysomes were observed in Δ*ccmL* mutants (Cai *et al.*, 2009;

Cameron *et al.*, 2013). Our data indicate that proper levels of expression of the different carboxysome proteins from stably integrated genes will be essential for the formation of carboxysomes with structures akin to those observed in cyanobacteria.

Overexpression of carboxysomal proteins as well as an absence of sufficient expression can also be inimical to the formation of proper microcompartments. Even when combinations of carboxysomal proteins gave rise to more than one type of structure, only a single morphological type was observed in each chloroplast, probably because of the particular level of expression of the carboxysomal proteins in each chloroplast. Elongated and disorganized structures were observed only in what appeared to be 'sick' chloroplasts (those with unusual chloroplast morphology). The circular, carboxysome-like structures were observed more frequently in chloroplasts with characteristic chloroplast morphology, probably because of a suitable level of expression of carboxysomal proteins.

We also observed round structures and elongated structures in plant material expressing CcmO-YFP, CcmK2 and CcmM58-YFP. These results raise two interesting issues. First, it suggests there is direct interaction between CcmM58 and the shell formed by CcmK2 and CcmO, as it is likely that such interaction gives the driving force to organize CcmO-YFP/CcmK2 sheets into round structures. This finding should not be surprising because a previous yeast two-hybrid experiment suggested the binding of CcmK2 to CcmM58 (Cot *et al.*, 2008); however, CcmN, which is also known to interact with CcmM58, has been shown to bind CcmK2 through a short C-terminal peptide, and is essential for recruiting the shell to the aggregation of Rubisco complexes with other components (Kinney *et al.*, 2012; Cameron *et al.*, 2013). If the CcmN is the main protein bridging the shell with other internal components, the interaction between CcmK2 and CcmM58 seems redundant. It is also possible that the lack of other stronger binding partners such as Rubisco, carbonic anhydrase and CcmN enables CcmM58 to interact with CcmK2. Second, although CcmL seems to play an essential role in the formation of circular microcompartments when it is co-expressed with CcmK2 and CcmO, it is not necessary when CcmM58 is also present. CcmL is believed to occupy the vertices of icosahedral-shaped carboxysomes, and the mostly elongated structures observed in the *ΔccmL* cyanobacteria supported such a role for CcmL (Cameron *et al.*, 2013); however, in the case of *α*-carboxysomes, the deletion of CcmL homologs did not disrupt their shapes (Cai *et al.*, 2009). Our results highlight the heterogeneity of structures that can arise from missing components. As most of the internal components were absent in our samples, it is possible that the structures observed arise from an assembly process that is completely different from a natural one.

Interestingly, we could not detect round structures or elongated assemblies in the samples co-expressing CcmN or CcmN17 with CcmK2 and CcmO. Although the fluorescence fusions indicated that CcmN and CcmN17 are able to co-localize with these shell proteins, the lack of formation of any specific structure suggests that CcmN by itself cannot arrange the shell components into more organized structures without CcmM58 or CcmL.

Bacterial microcompartments, including carboxysomes, have been proposed for biotechnological applications in synthetic biology and metabolic engineering because of their unique abilities to enclose specific enzymatic pathways (Corchero and Cedano, 2011; Frank *et al.*, 2013). Short N-terminal peptides from several internal components of propanediol utilization microcompartment (Pdu MCP) from *Salmonella enterica* have been demonstrated to be able to encapsulate foreign proteins such as GFP, glutathione-*S*-transferase and maltose-binding protein within Pdu MCP (Fan *et al.*, 2010, 2012; Fan and Bobik, 2011). A similar shell-targeting signal sequence was also reported to target EGFP and *β*-galactosidase to the recombinant ethanolamine utilization (eut) bacterial microcompartment shell proteins expressed in *Escherichia coli* (Choudhary *et al.*, 2012). Recently, a homologous 17-amino-acid peptide located at the C terminus of CcmN has been identified that can interact with CcmK2 in a similar fashion (Kinney *et al.*, 2012). Here, we showed that CcmN was able to co-localize with CcmK2 and CcmO-YFP in chloroplasts through the same C-terminal peptide (CcmN17). In addition, our work also demonstrates that the CcmN17 signal sequence alone is able to cause co-localization of a foreign protein, YFP, with the carboxysomal shell proteins, CcmK2 and CcmO, inside the chloroplasts. The results in our study present an exciting potential of *β*-carboxysome shells for synthetic biology and biotechnological applications in higher plants.

The current work describes the recombinant heterologous expression of *β*-carboxysomal proteins in higher plant chloroplasts. Previously, the propanediol utilization microcompartment from *Citrobacter freundii* and ethanolamine utilization microcompartment from *Salmonella enterica* have been successfully engineered in *E. coli* (Parsons *et al.*, 2008, 2010; Choudhary *et al.*, 2012). Bonacci *et al.* heterologously produced *α*-carboxysomes from *Halothiobacillus neapolitanus* in *E. coli* and demonstrated that the recombinant microcompartments were capable of fixing CO_2 (Bonacci *et al.*, 2012). By expressing CcmO-YFP and CcmK2 in combination with CcmL-YFP and/or CcmM58-YFP, we observed discrete structures with characteristics similar to *β*-carboxysomes. Therefore, this work provides evidence that specific combinations of carboxysomal proteins can assemble within the chloroplast stroma. These experiments are the first step towards the expression of a complete cyanobacterial carboxysome-based carbon-

concentrating mechanism in vascular plants, in order to enhance photosynthetic performance.

EXPERIMENTAL PROCEDURES

Plant expression vector construction

The *Synechococcus elongatus* PCC7942 *ccmK2*, *ccmL* and *ccmO* genes were amplified from *E. coli* expression vectors containing the respective coding regions, kindly provided by Cheryl Kerfeld (Michigan State University). Synthetic *ccmN*, *ccmM58*, *ccmK3*, *ccmK4* and *yfp* genes, designed to mimic the codon usage of the chloroplast protein expression system, were synthesized by Bioneer (http://www.bioneer.com). Each carboxysomal gene was fused with the chloroplast transit peptide from the Arabidopsis *recA* gene (Köhler *et al.*, 1997).

Table S1 contains the primers used in the overlap extension PCR procedure (Horton *et al.*, 1989) to generate the ctp::ccm gene fusion constructs with Phusion High-Fidelity DNA polymerase (Thermo Scientific, http://www.thermoscientific.com). The PCR products were first cloned into pCR8/GW/TOPO TA vector (Life Technologies, http://www.lifetechnologies.com) and subsequently transferred to the pEXSG-YFP Gateway destination vector, which has the tandem CaMV *35S* promoter (P35SS) and the YFP or CFP gene placed 5′ and 3′ of the Gateway recombination cassette, respectively (Jakoby *et al.*, 2006), through a standard Gateway® LR recombination reaction. Thus, each resulting vector contains a carboxysomal gene driven by P35SS, fused to the YFP or CFP gene at the 3′ end, as shown in Figure S4(a).

In order to express one or two additional carboxysomal genes from single vectors, nuclear expression operons driven by ubiquitin-10 (Puq10) and MAS (Pmas) promoters (Langridge *et al.*, 1989; Grefen *et al.*, 2010) were constructed with the overlap extension PCR procedure using the primers listed in Table S1. These operons were then inserted into the *Asc*I site located 5′ of the tandem CaMV *35S* promoter in the pEXSG-YFP vectors (Figure S4b). The attB2 segment located between the carboxysomal gene and the YFP or CFP gene in these vectors gives rise to a 15-amino-acid Gateway linker peptide (KGEFDPAFLYKVVDG) upon translation, which should provide sufficient separation between the carboxysomal protein domains and the fluorescent domain. In operons driven by the ubiquitin-10 or MAS promoter, we added a 9- or 12-amino-acid flexible linker peptide made up of GGS repeats between the YFP and carboxysomal proteins in order to minimize the influence of the YFP fusion on the molecular interactions among carboxysomal proteins. The expression vectors created in this work and their features are summarized in Table 1. The YFP and CFP used in this study are EYFP and mCerulean versions, and their amino-acid sequences are included in Data S1.

Each expression vector was electroporated into *Agrobacterium tumefaciens* GV3101/pMP90RK (Koncz and Schell, 1986) and transformants were selected on LB agar plates containing carbenicillin, kanamycin and gentamycin.

Transient expression of carboxysomal proteins in *Nicotiana benthamiana*

For transient expression of carboxysomal proteins in *N. benthamiana* leaf tissues, agroinoculation was performed as described previously (Sparkes *et al.*, 2006). About 5 ml of each agrobacterial culture grown to the late log phase was pelleted, re-suspended in 10 mM 2-(*N*-morpholine)-ethanesulphonic acid (MES) buffer, pH 5.6, with 10 mM MgCl$_2$ and 150 μM acetosyringone to an optical density of 0.3–0.5, and incubated in the dark at 28°C for 2–5 h.

Leaves from 4–6-week-old *N. benthamiana* plants grown at 10 h of light per day at ~50 μmol m^{-2} sec^{-1} of light intensity, at around 22°C, were infiltrated with the agrobacterial suspension on the abaxial side using a needle-less syringe. In some cases, a suspension of agrobacteria carrying the gene for the p19 protein of tomato bushy stunt virus (TBSV) was also co-infiltrated to improve the expression levels and duration of carboxysomal proteins (Voinnet *et al.*, 2003). Within 2–4 days after agroinfiltration, the leaf tissues were examined with a confocal microscope or fixed for immunogold labeling and transmission electron microscopy, as described below.

Confocal microscopy

Laser scanning confocal microscopy was performed on a Zeiss LSM 710 confocal microscope through a 25× multi-immersion objective. The 458-, 488- and 514-nm lines of an argon laser were used to excite CFP, chlorophyll and YFP, respectively. All the imaging experiments were carried out in sequential mode in order to minimize the spectral bleed-through from undesired fluorophores. The images were collected and processed with either ZEN 2009 or 2010 microscope software (Carl Zeiss Microscopy, http://www.zeiss.com/microscopy).

Chemical fixation, dehydration and embedding

Sections of leaf tissue 2 × 2 mm were excised from leaves using a sterile razor blade and incubated in primary fixative (2.5% glutaraldehyde, 4% paraformaldehyde in 0.05 M phosphate buffer, pH 7.2) for 2 h in low vacuum, over ice, with rotation. The samples were washed three times in 0.05 M phosphate buffer, pH 7.2,

Table 1 The plant expression vectors with β-carboxysomal genes created in this study

Vectors	Promoters and proteins to be expressed[a]
pEXSG-K2-YFP	P35SS – CcmK2-YFP
pEXSG-O-YFP	P35SS – CcmO-YFP
pEXSG-L-YFP	P35SS – CcmL-YFP
pEXSG-M58-YFP	P35SS – CcmM58-YFP
pEXSG-O-YFP -UK2	P35SS – CcmO-YFP, Puq10 – CcmK2
pEXSG-O-YFP -UL	P35SS – CcmO-YFP, Puq10 – CcmL
pEXSG-O-YFP -UK3	P35SS – CcmO-YFP, Puq10 – CcmK3
pEXSG-O-YFP -UK4	P35SS – CcmO-YFP, Puq10 – CcmK4
pEXSG-O-YFP -UK2-UL	P35SS – CcmO-YFP, Puq10 – CcmK2, Puq10 – CcmL
pEXSG-N-CFP	P35SS – CcmN-CFP
pEXSG-N-CFP-UK2-PmO-YFP	P35SS – CcmN-CFP, Puq10 – CcmK2, Pmas – CcmO-YFP
pEXSG-Nd17-CFP-UK2-PmO-YFP	P35SS – CcmNd17-CFP, Puq10 – CcmK2, Pmas – CcmO-YFP
pEXSG-N17-CFP-PmK2-UO-YFP	P35SS – CcmN17-CFP, Pmas – CcmK2, Puq10 – CcmO-YFP
pEXSG-YFP-N17	P35SS – YFP-CcmN17
pEXSG-O-CFP-PmK2-UYFP-N17	P35SS – CcmO-CFP, Pmas – CcmK2, Puq10 – YFP-CcmN17
pEXSG-YFP-N17-UO-PmK2	P35SS – YFP-CcmN17, Puq10 – CcmO, Pmas – CcmK2
pEXSG-YFP-Nd17-UO-PmK2	P35SS – YFP-CcmNd17, Puq10 – CcmO, Pmas – CcmK2

[a]P35SS, tandem *35S* promoter; Puq10, ubiquitin-10 promoter; Pmas, MAS promoter.

and then incubated in the second fixative (1% osmium tetroxide in 0.05 M phosphate buffer, pH 7.2) for 4 h over ice with rotation. The tissue was washed in 0.05 M phosphate buffer, pH 7.2, to remove all trace of osmium tetroxide and dehydrated through an acetone series, 30, 50, 70 and 90% (v/v) acetone in water (10 min each incubation), and then three times in 100% dry acetone (30 min each incubation), all at 20°C. Finally, the samples were embedded through increasing concentration of Spürr resin (TAAB), 30, 50, 70 to 100% v/v of resin in acetone, and then polymerized overnight at 60°C (Hulskamp *et al.*, 2010).

Cryofixation using a high pressure freezer, freeze substitution and embedding

Disks of leaf tissue (5 mm in diameter) were taken using a punch and then incubated in 150 mM sucrose for 8 min under low vacuum, in order to fill the intercellular spaces. The disks were transferred to the cavity of Leica Microsystems (http://www.leica-microsystems.com/) aluminum Type B Specimen carriers that are 6.0 × 0.5mm, pre-coated with 1-hexadecene and containing 150 mM sucrose as cryo-protectant. One side of the planchette is flat and there is a cylinder-shaped indentation on the other side of 5 × 0.3mm. The flat side of a second carrier was used as a lid. This plant material was then cryo-fixed using a high-pressure freezer unit at a rate of 20 000 Kelvins/sec (EM HPM100; Leica Microsystems).

For the second step of freeze substitution, the HPF tissue was transferred to 5-ml plastic pots containing a solution of 0.5% uranyl acetate in dry acetone pre-cooled in liquid nitrogen. The freeze substitution process was carried out in an EM AFS unit (Leica Microsystems) at −85°C for 48 h, followed by a linear warm up to −60°C for 5 h. After 1 h, samples were washed using dry ethanol to remove all trace of uranyl acetate. The samples were then infiltrated at low temperature using Lowicryl HM20 resin (Polysciences, http://www.polysciences.com). This step was performed at −60°C by increasing the concentration of resin, from 30, 50, 70 to 100% v/v HM20, in dry ethanol, with 1 h for each incubation. Finally, the samples were transferred to aluminium moulds and polymerized at −50°C for 24 h using a UV lamp (Hillmer *et al.*, 2012).

Immunogold labeling

Ultrathin sections (60–90 nm) were cut from the polymerised blocks on a Reichert–Jung Ultrmicrotome, and collected on gold grids. These were incubated in blocking solution (1% w/v BSA in PBS buffer) for 1 h, and then treated for 1 h with a blocking solution containing the primary antibody. Different primary antibodies against GFP (rabbit polyclonal to GFP; abcam, http://www.abcam.com) and different carboxysomal proteins were tested: rabbit polyclonal antibodies against CcmK2, CcmO, CcmM, CcmN and cyanobacterial Rubisco (Cambridge Research Biochemicals, http://www.crbdiscovery.com). The grids carrying the sections were washed three times in blocking solution and then incubated for 1 h in blocking solution containing a secondary antibody conjugated with 10-nm gold particles (goat polyclonal antibody to rabbit IgG, 10-nm gold conjugated; abcam). The excess of secondary antibody was removed by washing three times in blocking solution and then washing three times in distilled water.

Transmission electron microscopy

Grids carrying ultrathin sections of both embedded samples, cryo-fixed and chemically fixed, were post stained using 2% (w/v) aqueous solution of uranyl acetate and lead citrate. Images were obtained using a transmission electron microscope JEM 2011 FasTEM Jeol UK operating at 200 kV, equipped with a Gatan Ultrascan 1000 CCD camera and a Gatan Dual Vision 300 CCD camera.

SUPPORTING INFORMATION

Additional Supporting Information may be found in the online version of this article.

Data S1. Synthesized genes.

Figure S1. Additional TEM images of leaf sections from agroinfiltrated *Nicotiana benthamiana* expressing CcmO-YFP, CcmK2 and CcmM58-YFP, or CcmO-YFP, CcmK2, CcmL and CcmM58-YFP.

Figure S2. Confocal images of leaf sections from agroinfiltrated *Nicotiana benthamiana* expressing CcmN17-CFP, CcmK2 and CcmO-YFP.

Figure S3. TEM images of leaf sections from agroinfiltrated *Nicotiana benthamiana* expressing CcmN-CFP, CcmK2 and CcmO-YFP, or YFP-CcmN17, CcmK2 and CcmO-YFP.

Figure S4. The schematic of agrobacterial expression vectors.

Table S1. The oligonucleotides used in the construction of plant expression vectors.

REFERENCES

Bobik, T.A. (2006) Polyhedral organelles compartmenting bacterial metabolic processes. *Appl. Microbiol. Biotechnol.* **70**, 517–725.

Bonacci, W., Teng, P.K., Afonso, B., Niederholtmeyer, H., Grob, P., Silver, P.A. and Savage, D.F. (2012) Modularity of a carbon-fixing protein organelle. *Proc. Natl Acad. Sci. USA* **109**, 478–483.

Cai, F., Menon, B.B., Cannon, G.C., Curry, K.J., Shively, J.M. and Heinhorst, S. (2009) The pentameric vertex proteins are necessary for the icosahedral carboxysome shell to function as a CO_2 leakage barrier. *PLoS ONE* **4**, e7521.

Cai, F., Sutter, M., Cameron, J.C., Stanley, D.N., Kinney, J.N. and Kerfeld, C.A. (2013) The structure of CcmP, a tandem bacterial microcompartment domain protein from the β-carboxysome, forms a subcompartment within a microcompartment. *J. Biol. Chem.* **288**, 16055–16063.

Cameron, J.C., Wilson, S.C., Bernstein, S.L. and Kerfeld, C.A. (2013) Biogenesis of a bacterial organelle: the carboxysome assembly pathway. *Cell*, **155**, 1131–1140.

Cannon, G.C., Bradburne, C.E., Aldrich, H.C., Baker, S.H., Heinhorst, S. and Shively, J.M. (2001) Microcompartments in prokaryotes: carboxysomes and related polyhedra. *Appl. Environ. Microbiol.* **67**, 5351–5361.

Chen, A.H., Robinson-Mosher, A., Savage, D.F., Silver, P.A. and Polka, J.K. (2013) The bacterial carbon-fixing organelle is formed by shell envelopment of preassembled cargo. *PLoS ONE* **8**, e76127.

Choudhary, S., Quin, M.B., Sanders, M.A., Johnson, E.T. and Schmidt-Dannert, C. (2012) Engineered protein nano-compartments for targeted enzyme localization. *PLoS ONE* **7**, e33342.

Corchero, J.L. and Cedano, J. (2011) Self-assembling, protein-based intracellular bacterial organelles: emerging vehicles for encapsulating, targeting and delivering therapeutical cargoes. *Microb. Cell Fact.* **10**, 92.

Cot, S.S., So, A.K. and Espie, G.S. (2008) A multiprotein bicarbonate dehydration complex essential to carboxysome function in cyanobacteria. *J. Bacteriol.* **190**, 936–945.

Fan, C.G. and Bobik, T.A. (2011) The N-terminal region of the medium subunit (PduD) packages adenosylcobalamin-dependent diol dehydratase (PduCDE) into the Pdu microcompartment. *J. Bacteriol.* **193**, 5623–5628.

Fan, C.G., Cheng, S.Q., Liu, Y., Escobar, C.M., Crowley, C.S., Jefferson, R.E., Yeates, T.O. and Bobik, T.A. (2010) Short N-terminal sequences package proteins into bacterial microcompartments. *Proc. Natl Acad. Sci. USA* **107**, 7509–7514.

Fan, C.G., Cheng, S.Q., Sinha, S. and Bobik, T.A. (2012) Interactions between the termini of lumen enzymes and shell proteins mediate enzyme encapsulation into bacterial microcompartments. *Proc. Natl Acad. Sci. USA* **109**, 14995–15000.

Frank, S., Lawrence, A.D., Prentice, M.B. and Warren, M.J. (2013) Bacterial microcompartments moving into a synthetic biological world. *J. Biotechnol.* **163**, 273–279.

Grefen, C., Donald, N., Hashimoto, K., Kudla, J., Schumacher, K. and Blatt, M.R. (2010) A ubiquitin-10 promoter-based vector set for fluorescent protein tagging facilitates temporal stability and native protein distribution in transient and stable expression studies. *Plant J.* **64**, 355–365.

Hillmer, S., Viotti, C. and Robinson, D.G. (2012) An improved procedure for low-temperature embedding of high-pressure frozen and freeze-substituted plant tissues resulting in excellent structural preservation and contrast. *J. Microsc.* **247**, 43–47.

Horton, R.M., Hunt, H.D., Ho, S.N., Pullen, J.K. and Pease, L.R. (1989) Engineering hybrid genes without the use of restriction enzymes - gene-splicing by overlap extension. *Gene* **77**, 61–68.

Hulskamp, M., Schwab, B., Grini, P. and Schwarz, H. (2010) Transmission electron microscopy (TEM) of plant tissues. *Cold Spring Harb. Protoc.* **2010**, Pdb prot4958.

Jakoby, M.J., Weinl, C., Pusch, S., Kuijt, S.J., Merkle, T., Dissmeyer, N. and Schnittger, A. (2006) Analysis of the subcellular localization, function, and proteolytic control of the Arabidopsis cyclin-dependent kinase inhibitor ICK1/KRP1. *Plant Physiol.* **141**, 1293–1305.

Kaneko, Y., Danev, R., Nagayama, K. and Nakamoto, H. (2006) Intact carboxysomes in a cyanobacterial cell visualized by hilbert differential contrast transmission electron microscopy. *J. Bacteriol.* **188**, 805–808.

Keeling, T.J., Samborska, B., Demers, R.W. and Kimber, M.S. (2014) Interactions and structural variability of β-carboxysomal shell protein CcmL. *Photosynth. Res.* [Epub ahead of print].

Kerfeld, C.A., Sawaya, M.R., Tanaka, S., Nguyen, C.V., Phillips, M., Beeby, M. and Yeates, T.O. (2005) Protein structures forming the shell of primitive bacterial organelles. *Science*, **309**, 936–938.

Kinney, J.N., Axen, S.D. and Kerfeld, C.A. (2011) Comparative analysis of carboxysome shell proteins. *Photosynth. Res.* **109**, 21–32.

Kinney, J.N., Salmeen, A., Cai, F. and Kerfeld, C.A. (2012) Elucidating essential role of conserved carboxysomal protein CcmN reveals common feature of bacterial microcompartment assembly. *J. Biol. Chem.* **287**, 17729–17736.

Köhler, R.H., Cao, J., Zipfel, W.R., Webb, W.W. and Hanson, M.R. (1997) Exchange of protein molecules through connections between higher plant plastids. *Science*, **276**, 2039–2042.

Koncz, C. and Schell, J. (1986) The promoter of TL-DNA gene 5 controls the tissue-specific expression of chimaeric genes carried by a novel type of Agrobacterium binary vector. *Mol. Gen. Genet.* **204**, 383–396.

Langridge, W.H.R., Fitzgerald, K.J., Koncz, C., Schell, J. and Szalay, A.A. (1989) Dual promoter of *Agrobacterium tumefaciens* mannopine synthase genes is regulated by plant-growth hormones. *Proc. Natl Acad. Sci. USA* **86**, 3219–3223.

Long, S.P. (1991) Modification of the response of photosynthetic productivity to rising temperature by atmospheric CO_2 concentrations: has its importance been underestimated? *Plant, Cell Environ.* **14**, 729–739.

Long, B.M., Price, G.D. and Badger, M.R. (2005) Proteomic assessment of an established technique for carboxysome enrichment from Synechococcus PCC7942. *Can. J. Bot.* **83**, 746–757.

Long, B.M., Tucker, L., Badger, M.R. and Price, G.D. (2010) Functional cyanobacterial β-carboxysomes have an absolute requirement for both long and short forms of the CcmM protein. *Plant Physiol.* **153**, 285–293.

Ludwig, M., Sültemeyer, D. and Price, G.D. (2000) Isolation of *ccmKLMN* genes from the marine cyanobacterium, *Synechococcus* sp. PCC7002 (Cyanophyceae), and evidence that CcmM is essential for carboxysome assembly. *J. Phycol.* **36**, 1109–1119.

McGrath, J.M. and Long, S.P. (2014) Can the cyanobacterial carbon-concentrating mechanism increase photosynthesis in crop species? A theoretical analysis *Plant Physiol.* **164**, 2247–2261.

Menon, B.B., Dou, Z., Heinhorst, S., Shively, J.M. and Cannon, G.C. (2008) *Halothiobacillus neapolitanus* carboxysomes sequester heterologous and chimeric RubisCO species. *PLoS ONE* **3**, e3570.

Parsons, J.B., Dinesh, S.D., Deery, E. *et al.* (2008) Biochemical and structural insights into bacterial organelle form and biogenesis. *J. Biol. Chem.* **283**, 14366–14375.

Parsons, J.B., Frank, S., Bhella, D., Liang, M.Z., Prentice, M.B., Mulvihill, D.P. and Warren, M.J. (2010) Synthesis of empty bacterial microcompartments, directed organelle protein incorporation, and evidence of filament-associated organelle movement. *Mol. Cell* **38**, 305–315.

Price, G.D., Howitt, S.M., Harrison, K. and Badger, M.R. (1993) Analysis of a genomic DNA region from the cyanobacterium *Synechococcus* Sp strain PCC7942 involved in carboxysome assembly and function. *J. Bacteriol.* **175**, 2871–2879.

Price, G.D., Sültemeyer, D., Klughammer, B., Ludwig, M. and Badger, M.R. (1998) The functioning of the CO_2 concentrating mechanism in several cyanobacterial strains: a review of general physiological characteristics, genes, proteins, and recent advances. *Can. J. Bot.* **76**, 973–1002.

Price, G.D., Badger, M.R., Woodger, F.J. and Long, B.M. (2008) Advances in understanding the cyanobacterial CO_2-concentrating-mechanism (CCM): functional components, Ci transporters, diversity, genetic regulation and prospects for engineering into plants. *J. Exp. Bot.* **59**, 1441–1461.

Price, G.D., Pengelly, J.J.L., Forster, B., Du, J.H., Whitney, S.M., von Caemmerer, S., Badger, M.R., Howitt, S.M. and Evans, J.R. (2013) The cyanobacterial CCM as a source of genes for improving photosynthetic CO_2 fixation in crop species. *J. Exp. Bot.* **64**, 753–768.

Rae, B.D., Long, B.M., Badger, M.R. and Price, G.D. (2012) Structural determinants of the outer shell of β-carboxysomes in *Synechococcus elongatus* PCC 7942: roles for Ccm K2, K3–K4, CcmO, and CcmL. *PLoS ONE* **7**, e43571.

Rae, B.D., Long, B.M., Badger, M.R. and Price, G.D. (2013) Functions, compositions, and evolution of the two types of carboxysomes: Polyhedral microcompartments that facilitate CO_2 fixation in cyanobacteria and some proteobacteria. *Microbiol. Mol. Biol. Rev.* **77**, 357–379.

Samborska, B. and Kimber, M.S. (2012) A dodecameric CcmK2 structure suggests β-carboxysomal shell facets have a double-layered organization. *Structure*, **20**, 1353–1362.

Sparkes, I.A., Runions, J., Kearns, A. and Hawes, C. (2006) Rapid, transient expression of fluorescent fusion proteins in tobacco plants and generation of stably transformed plants. *Nat. Protoc.* **1**, 2019–2025.

Tanaka, S., Kerfeld, C.A., Sawaya, M.R., Cai, F., Heinhorst, S., Cannon, G.C. and Yeates, T.O. (2008) Atomic-level models of the bacterial carboxysome shell. *Science*, **319**, 1083–1086.

Tanaka, S., Sawaya, M.R., Phillips, M. and Yeates, T.O. (2009) Insights from multiple structures of the shell proteins from the β-carboxysome. *Protein Sci.* **18**, 108–120.

Voinnet, O., Rivas, S., Mestre, P. and Baulcombe, D. (2003) An enhanced transient expression system in plants based on suppression of gene silencing by the p19 protein of tomato bushy stunt virus. *Plant J.* **33**, 949–956.

Whitney, S.M., Houtz, R.L. and Alonso, H. (2011) Advancing our understanding and capacity to engineer nature's CO_2-sequestering enzyme, Rubisco. *Plant Physiol.* **155**, 27–35.

Yeates, T.O., Kerfeld, C.A., Heinhorst, S., Cannon, G.C. and Shively, J.M. (2008) Protein-based organelles in bacteria: carboxysomes and related microcompartments. *Nat. Rev. Microbiol.* **6**, 681–691.

Yeates, T.O., Thompson, M.C. and Bobik, T.A. (2011) The protein shells of bacterial microcompartment organelles. *Curr. Opin. Struct. Biol.* **21**, 223–231.

Zarzycki, J., Axen, S.D., Kinney, J.N. and Kerfeld, C.A. (2013) Cyanobacterial-based approaches to improving photosynthesis in plants. *J. Exp. Bot.* **64**, 787–798.